Scanning Microscopy

Volume 8 | Number 3 Article 23

8-5-1994

Ultrastructural Patterns of Cell Damage and Death Following Gamma Radiation Exposure of Murine Erythroleukemia Cells

R. Di Pietro
Istituto di Morfologia Umana

E. Falcieri
Istituto di Morfologia Umana

L. Centurione
Istituto di Morfologia Umana

M. A. Centurione
Istituto di Citomorfologia Normale e Patologica

G. Mazzotti
Istituto di Anatomia Umana Normale

See next page for additional authors

Ultrastructural Patterns of Cell Damage and Death Following Gamma Radiation Exposure of Murine Erythroleukemia Cells

Authors

R. Di Pietro, E. Falcieri, L. Centurione, M. A. Centurione, G. Mazzotti, and R. Rana

Scanning Microscopy, Vol. 8, No. 3, 1994 (Pages 667-673) 0891-7035/94$5.00+.25
Scanning Microscopy International, Chicago (AMF O'Hare), IL 60666 USA

ULTRASTRUCTURAL PATTERNS OF CELL DAMAGE AND DEATH FOLLOWING GAMMA RADIATION EXPOSURE OF MURINE ERYTHROLEUKEMIA CELLS

R. Di Pietro*, E. Falcieri, L. Centurione, M.A. Centurione[1], G. Mazzotti[2] and R. Rana

Istituto di Morfologia Umana, Via dei Vestini, 6, 66100 Chieti, Italy;
[1]Istituto di Citomorfologia Normale e Patologica, CNR, Via dei Vestini, 6, 66100 Chieti, Italy;
[2]Istituto di Anatomia Umana Normale, Via Irnerio, 48, 40126 Bologna, Italy.

(Received for publication February 4, 1994 and in revised form August 5, 1994)

Abstract

Radiation causes damage to cell surface membranes, cytoplasmic organelles, and the nuclear process of DNA synthesis and repair, and this eventually results in different modes of cell death. In this study we examined murine erythroleukemia (MEL) cells, exposed to 15 and 60 Gy of 10 MeV photonic energy, and left in culture for up to 96 hours. Electron microscopical analysis was performed on conventionally embedded samples and freeze-fracture replicas, in order to detect ultrastructural patterns of cell damage and death. Of interest was the observation of chromatin condensates, nuclear membrane associations and nuclear pore redistribution during early apoptosis. Pronounced rearrangements of transmembrane particles during late stages of cellular necrosis were also found. The morphological damage induced by both doses of radiation as a function of time after exposure was only quantitatively but not qualitatively different.

Key Words: Gamma radiation, radiation damage, high-dose radiation exposure, cell death, apoptosis, necrosis, electron microscopy, freeze fracture, murine erythroleukemia cells, Friend cells.

*Address for correspondence:
Roberta Di Pietro
Istituto di Morfologia Umana Normale,
Via dei Vestini,
66100 Chieti, Italy
Telephone number: +39-871-355242
FAX number: +39-871-574361

Introduction

In recent years several authors have been interested in the biological effects of ionizing radiation, due to the frequent use of this type of radiation in cancer therapy [4, 15]. Radiation is known to cause damage to cellular membranes by altering carbohydrate composition [8] and membrane permeability [12]. This involves changes in polyphosphoinositide metabolism [13], protein kinase C activity and calcium (Ca^{2+}) uptake [9], which precede the activation of a Ca^{2+}-dependent nuclear endonuclease, recently identified as DNAse I [11], responsible for the fragmentation of nuclear DNA into oligonucleosomal subunits typical of death by apoptosis [20]. Apoptosis is a physiologic mode of cell death because it represents a metabolically active process of "cell suicide" that occurs normally during embryogenesis, metamorphosis and hormone-dependent tissue atrophy [5, 21]. Irradiation, chemotherapy and hormone-therapy all induce apoptosis also in tumor cells. Apoptosis is not the only mode of cell death; the alternative is cellular necrosis [6, 15]. Recently we described the dose- and time-dependence of the morphological damage following low- and high-dose radiation exposure of human peripheral blood lymphocytes [13]. In fact, high-dose damage was immediately detectable after exposure while low-dose damage, initially undetectable, became qualitatively similar to high-dose damage during the time post irradiation. In this study, we have therefore evaluated type and amount of acute and long-term morphological damage in murine erythroleukemia (MEL) cells exposed to gamma radiation. The analysis was carried out by transmission electron microscopy on ultrathin sections and freeze fracture replicas. The freeze fracture technique, in fact, allows a detailed analysis of cell surfaces at high resolution and is the method of choice for the study of organellar and plasma membranes.

Materials and Methods

Cell culture and irradiation protocol

Murine Friend erythroleukemia cells (FLC-745) were grown in RPMI 1640 medium supplemented with

10% fetal calf serum and 2 mM L-glutamine in a 5% CO_2 atmosphere. Plastic Falcon flasks containing exponentially growing cells (1 x 10^6/ml) in a total volume of 250 ml of fresh medium were exposed at room temperature to 15 and 60 Gy, dose rate 3 Gy/min, administered by a Mevatron 74 Siemens linear accelerator (photonic energy: 10 MeV).

Control unirradiated samples were kept at room temperature for the same period of irradiation. Both irradiated and unirradiated cells were then incubated at 37°C, in the presence of CO_2, for 0, 18, 24, 48 and 96 hours and used for morphological assays.

Cell viability was checked by means of the blue trypan exclusion test.

Conventional electron microscopy

Cell pellets were fixed with 2.5% glutaraldehyde in 0.1 M phosphate buffer pH 7.2 for 45 minutes at 4°C, rinsed in the same buffer and then processed for conventional Spurr embedding. Semi-thin sections were cut to count different morphological patterns in light microscopy with a Zeiss light microscope. Thin sections were stained with uranyl acetate and lead citrate and observed with a Zeiss 109 transmission electron microscope.

Freeze-fracture

Identically fixed specimens were cryo-protected with 30% glycerol in 0.1 M phosphate buffer for 30 minutes. They were then mounted on gold supports, quickly frozen in Freon 22, transferred into liquid nitrogen and fractured in a Balzers BAF 400 D device at -115°C. Shadowing was carried out with 2 nm of platinum-carbon at 45°, immediately followed by 25 nm of carbon at 90°. In both cases, the thickness was controlled by a quartz crystal film monitor. The replicas were cleaned for 30 minutes in undiluted commercial bleach and degreased by floating them in a 2:1 chloroform:methanol mixture. Folding was prevented by carefully adding a few drops of distilled water. After rinsing in distilled water, the replicas were collected on Formvar carbon-coated nickel grids [3]. The observations were carried out on a Philips CM 10 transmission electron microscope.

Statistics

Experimental data are expressed as mean percentage ± standard deviation (S.D.). Comparisons were made by means of the Student two-tailed t-test. Values of $p < 0.05$ were considered significant.

Results

Ultrastructural analysis showed different morphological patterns of cell damage and death induced by ionizing radiation exposure. Among these, the most common and easily quantifiable were multinucleate cells, displaying 3 or more nuclei, (classified as MN), apoptotic cells, recognizable by their typical nuclear features and cytoplasmic condensation in the presence of good organelle preservation (classified as A) and necrotic cells, identified by the swelling/progressing to the total disintegration of organized cell structure (classified as N). As shown in Figure 1 and Table 1, at time 0 there were no significant differences between control and irradiated samples in the percentage of the three parameters considered (MN, A, N). Within 18 hours of irradiation, the percentage of necrotic cells did not significantly differ in control and irradiated samples, whereas the percentage of apoptotic cells was significantly ($p < 0.05$) greater in irradiated samples and mainly after the higher dose. After 24 and 48 hours, there was a progressive increase in the necrosis, especially after 60 Gy, while the apoptosis seemed to have reached a plateau. Finally, irradiated samples left 96 hours in culture, displayed completely aberrant patterns with the highest percentage of multinucleate and necrotic cells, especially after the higher dose.

Different ultrastructural patterns are shown in Figures 2 and 3. At time 0, after 60 Gy exposure, various degrees of damage were observed (not shown) both in the nucleus (partial heterochromatin decondensation and multiple indentations) and in the cytoplasm (mitochondrial crest disorganization and, occasionally, vacuolization). After 15 Gy, a smaller number of cells showed the same type of damage. From 18 hours onwards in post-irradiation cultures, an increasing number of cells was affected by mitochondrial swelling and polymorphism, cytoplasmic inclusions, flakes, diffuse vacuolization and lately nuclear pyknosis, preceding the total disruption and disintegration of cellular membranes, typical hallmarks of cellular necrosis (Fig. 2). Cell membrane lesions of late stages of cellular necrosis appeared as pronounced rearrangements of transmembrane particles in freeze-fracture replicas (Fig. 3). In contrast, a certain number of cells displayed chromatin condensation and irregular distribution of the nuclear pores (Figs. 2 and 3); this was identified as early apoptosis. Nuclear pores, which were absent in the parts of the nuclear membrane delineating compact chromatin areas, were widely distributed and in close contact with each other in those parts of the nuclear membranes corresponding to decondensed nuclear areas. In the following stage (18 hours), characteristic cap-shaped chromatin areas and highly electron dense micronuclei containing compact chromatin were detected (Figs. 2 and 3). In spite of these alterations, the plasma membrane and cytoplasmic morphology looked well preserved. Only at late stages nuclear fragmentation was followed by a slight cytoplasm hydration probably preceding a final "secondary necrosis".

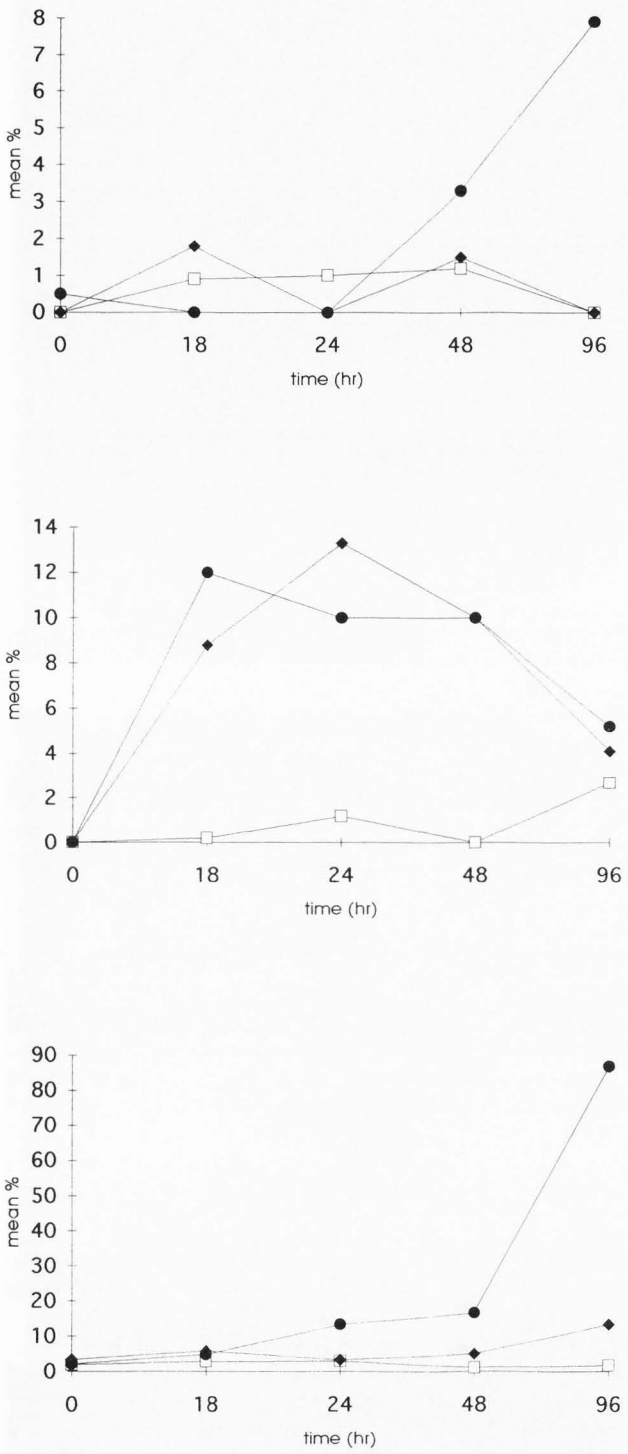

Figure 1. Mean percentage of multinucleate (**top**), apoptotic (**middle**) and necrotic (**bottom**) cells in unirradiated control (hollow squares), and 15 Gy (solid diamonds) and 60 Gy (solid circles) irradiated samples.

Table 1. Mean percentages ± standard deviation of morphological patterns at different time intervals in post-irradiation culture. Data refer to 100 cells scored for each of the three separate determinations.

Time (hrs.)	MN	A	N
	Unirradiated		
0	0	0	2.0 ± 0.7
18	0.9 ± 0.2	0.2 ± 0.1	2.9 ± 0.5
24	1.0 ± 0.3	1.2 ± 0.5	3.0 ± 0.3
48	1.2 ± 0.8	0	1.2 ± 0.9
96	0	2.7 ± 0.5	1.8 ± 0.6
	15 Gy		
0	0	0	3.5 ± 0.8
18	1.8 ± 0.6	8.8 ± 2.5*	5.8 ± 2.7
24	0	13.3 ± 3.4*	3.3 ± 1.0
48	1.5 ± 0.4	10.0 ± 3.3*	5.0 ± 0.9
96	0	4.1 ± 1.2	13.3 ± 2.0*
	60 Gy		
0	0.5 ± 0.1	0	2.2 ± 0.7
18	0	12.0 ± 2.3*	4.8 ± 1.2
24	0	10.0 ± 2.4*	13.3 ± 6.1
48	3.3 ± 0.9	10.0 ± 2.6*	16.6 ± 4.2
96	7.9 ± 1.9	5.2 ± 1.4	86.8 ± 6.4**

MN: multinucleate; A: apoptosis; N: necrosis;
*$p < 0.05$; **$p < 0.001$.

Discussion

In previous studies, morphological alterations have been detected in a number of irradiated animal tumors [1, 21]. Major changes include decreased cellularity, reduced mitotic activity, increased cell and nuclear size, metaplasia and changes in differentiation [1, 2, 19]. Both necrosis and apoptosis have been reported after ionizing radiation exposure, but only the latter has been considered as an early radiation effect [15].

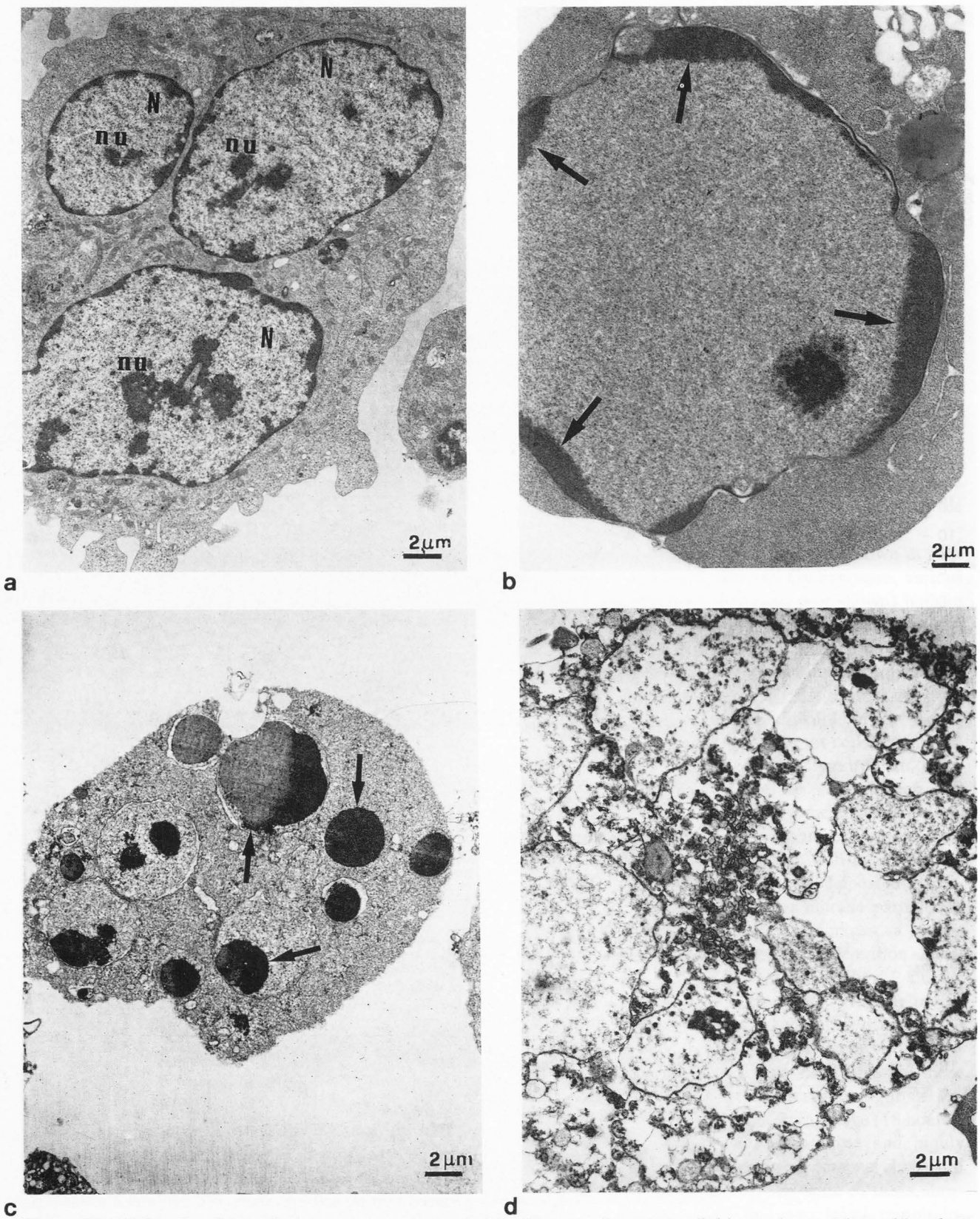

Figure 2. MEL cells after radiation exposure: transmission electron microscopy of thin sections. (**a**): multinucleate cell with a regular nuclear arrangement (N), nu: nucleolus; (**b**): early apoptosis: note the typical chromatin margination (arrows); (**c**): late apoptosis showing electron dense micronuclei (arrows) surrounded by the nuclear envelope; (**d**): necrotic cell with complete disruption of normal architecture.

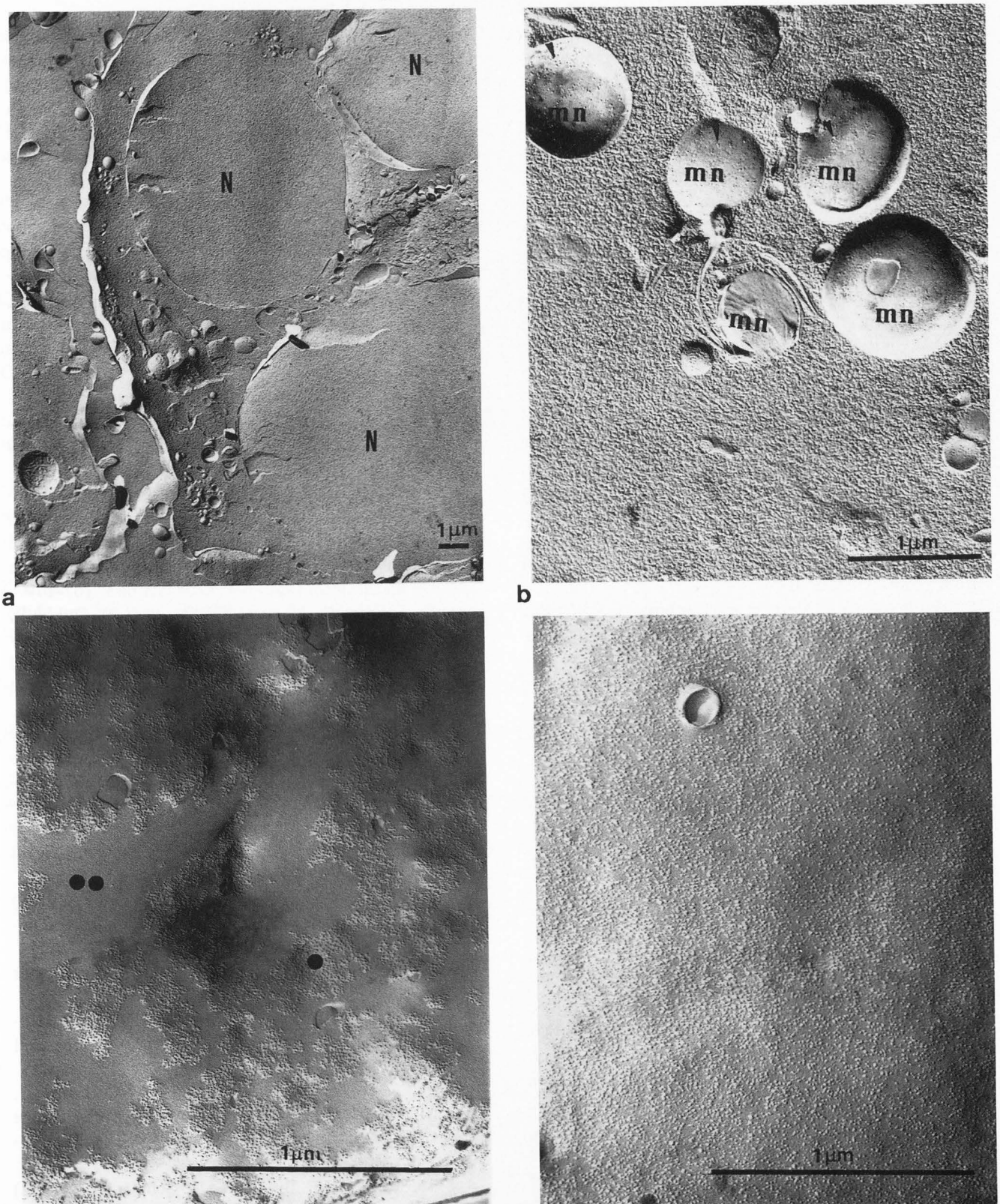

Figure 3. MEL cells after radiation exposure: freeze fracture replicas. (**a**): multinucleate cell, N: nucleus; (**b**): late apoptosis: mn: micronuclei, irregular distribution of the nuclear pores (arrowheads); (**c**): profoundly rearranged membrane architecture of a necrotic cell: ● clusters of intramembrane particles for ion transport; ●● regions lacking intramembrane particles; (**d**): cell plasma membrane P face (protoplasmic face) of unaffected cells.

In this study, high single doses of ionizing radiation (15 and 60 Gy) were administered to induce severe damage in a great number of cells. Friend erythroleukemia cells were chosen as experimental model in an attempt to correlate morphological data with previous biochemical findings [13] of an early involvement of polyphosphoinositide metabolism after radiation exposure (time 0) and a subsequent peak (time 18 hours) in the activity of DNA beta polymerase, known as the main repair enzyme.

According to light microscopy, whatever the dose, at time 0 as well as 18, 24 and 48 hours after irradiation a great number of cells was still apparently well preserved, while at 96 hours after the higher dose all the cells were completely aberrant, confirming our previous findings about the time- and dose-dependence of the morphological damage [14]. In fact, while after the higher dose the cells could not grow and proliferate for over 96 hours, after the lower dose they could grow in culture for over two weeks (data not shown). It is worth noting, however, that the high percentage of necrotic cells found 96 hours after the higher dose was mainly due to late apoptotic stages, not easily distinguishable from primary necrosis.

With regard to electron microscopy, two different stages of apoptosis were observed after radiation exposure:

1) **Early apoptosis**: This is characterized by a largely intact cell membrane and cytoplasmic organelles, micronuclei and typical chromatin condensation into dense granular caps close to the nuclear membrane [12, 17, 20]; in the areas of the nuclear membrane corresponding to these dense granular caps, nuclear pores were absent, as confirmed by freeze-fracture analysis, which showed their irregular distribution on the nuclear surface (unpublished observations).

2) **Late apoptosis**: This is characterized by a number of small membrane-bounded fragments in various stages of degradation with intensely stained and featureless cytoplasm [20].

Besides **necrosis**, electron microscopy documented the finding of **multinucleate cells**, showing more than two nuclei of different shape and size, evident nucleoli and chromatin decondensation. It had previously been demonstrated that this pattern was an effect of radiation therapy and cytotoxic drugs [15].

All in all, our observations show that apoptosis is easily and early detectable, dose-dependent and possibly stable for a long period before progressing to necrosis. The apparent discrepancies with some findings of higher frequencies of apoptotic cells after lower doses [10, 18] or just a few hours after irradiation [16] make further investigations of this phenomenon in this particular cell system necessary. However, a possible explanation could be the existence of different forms of apoptosis (protein- and RNA synthesis-dependent or independent [7]). Also, in different models, commitment to apoptotic death could take place at different points in the cell cycle, or at different points related to DNA repair capability [7].

Acknowledgments

The authors wish to thank Dr. G. Sanità Di Toppi (Health Physicist USL 04 Chieti, Radiotherapy, Nuclear Medicine) for the assessment of the irradiation protocol. This work was supported by Italian MPI Grant 60% 1992.

References

1. Allan DJ, Gobe GC, Harmon BV (1988) Sertoli cell death by apoptosis in the immature rat testis following X-irradiation. Scanning Microsc **2**, 503-512.

2. Bayreuther K, Francz PI, Gogol J, Kontermann K (1992) Terminal differentiation, aging, apoptosis, and spontaneous transformation in fibroblast stem cell system in vivo and in vitro. Ann NY Acad Sci **663**, 167-179.

3. Falcieri E, Mariani AR, Mariani E, Gobbi P, Facchini A, Manzoli FA (1990) A morphological study of membrane lesions during Natural Killer-mediated lysis. J Submicrosc Cytol Pathol **22**, 191-202.

4. Garvy BA, Telford WG, King LE, Fraker PJ. (1993). Glucocorticoids and irradiation-induced apoptosis in normal murine bone marrow B-lineage lymphocytes as determined by flow cytometry. Immunology **79**, 270-277.

5. Kerr JFR, Searle J, Harmon BV, Bishop CJ. (1987). Apoptosis. In: Perspectives on Mammalian Cell Death. Potten CS (ed.). Oxford Univ Press, UK. p. 93.

6. Laster SM, Wood JG, Gooding LR (1988) Tumor necrosis factor can induce both apoptotic and necrotic forms of cell lysis. J Immunol **141**, 2629-2634.

7. Martin SJ (1993) Apoptosis: suicide, execution or murder? Trends Cell Biol **3**, 141-144.

8. Nievergelt-Egido MC, Bain M (1992) Cell surface alterations by X-rays. In: Proc 5th Int Congr Cell Biol. Academic Press, London, UK. p. 151 (abstract).

9. Ojeda F, Guarda Ml, Malobuado C, Folch H, Diehl H (1992) Role of protein Kinase C in thymocyte apoptosis induced by irradiation. Int J Rad Biol **61**, 663-667.

10. Payne CM, Bjore CG Jr, Schultz DA (1992) Change in the frequency of apoptosis after low- and high-dose X-irradiation of human lymphocytes. J Leuk Biol **52**, 433-440.

11. Peitsch MC, Polzar B, Stephan H, Crompton T, MacDonald HR, Mannhers HG, Tschopp J (1993) Char-

acterization of the endogenous deoxyribonuclease involved in nuclear DNA degradation during apoptosis (programmed cell death). EMBO J **12**, 371-377.

12. Ramakrishnan N, McClain DE, Catravas GN. (1993). Membranes as sensitive targets in thymocyte apoptosis. Int J Radiat Biol **63**, 693-701.

13. Rana R, Vitale M, Mazzotti G, Manzoli L, Papa S (1990). Radiosensitivity of human Natural Killer cells: binding and cytotoxic activities of natural killer cell subsets. Radiat Res **124**, 96-102.

14. Rana R, Cataldi A, Di Pietro R, Mazzotti G, Centurione L, Robuffo I, Vitale M, Miscia S (1994) Intranuclear signalling system: inositol lipid involvement in cell repair processes upon ionizing radiation exposure. Cell Signal **6**, 475-480.

15. Stephens LC, Ang KK, Schultheiss TE, Milas L, Meyn RE (1991) Apoptosis in irradiated murine tumors. Radiat Res **127**, 308-316.

16. Stephens LC, Hunter NR, Ang KK, Milas L, Mayn RE (1993) Development of apoptosis in irradiated murine tumors as a function of time and dose. Radiat Res **135**, 75-80.

17. Vitale M, Zamai L, Mazzotti G, Cataldi A, Falcieri E (1993) Differential kinetics of propidium iodide uptake in apoptotic and necrotic thymocytes. Histochemistry **100**: 223-229.

18. Williams GT (1992) Programmed cell death: apoptosis and oncogenesis. Cell **65**, 1097-1098.

19. Wyllie AH (1993) Apoptosis (The 1992 Frank Rose Memorial Lecture). Br J Cancer **67**, 205-208.

20. Wyllie AH, Morris RG, Smith AL, Dunlop D. (1984). Chromatin cleavage in apoptosis: association with condensed chromatin morphology and dependence on macromolecular synthesis. J Pathol **142**, 67-77.

Discussion with Reviewers

T.M. Seed: Samples were irradiated at room temperature for considerable periods of time (20 minutes in the case of the 60 cGy dose). Do the authors feel that repair functions during the exposure period might have influenced the noted apoptotic response patterns?

Authors: We cannot properly answer this interesting question which presumes the parallel assay of DNA polymerases and morphological patterns in the few hours after irradiation. In a previous study [13], we found an increase in DNA beta polymerase activity within the first hour in postirradiation culture and a peak of this activity after 18 hours, which was related to the increase in bromodeoxyuridine (BrdU) incorporation. In addition, a uniform model is required, which is not the case in our system because the cells are in different metabolic conditions. Very few data are yet available about the cell cycle phase related to apoptosis triggering and a study on synchronized cells is therefore planned.